

# Easing Tensions with Quartessence

Stefano Camera<sup>a,b,c,d</sup>, Matteo Martinelli<sup>e</sup>, Daniele Bertacca<sup>f</sup>

<sup>a</sup>*Dipartimento di Fisica, Università degli Studi di Torino, Via P. Giuria 1, 10125 Torino, Italy*

<sup>b</sup>*INFN, Sezione di Torino, Via P. Giuria 1, 10125 Torino, Italy*

<sup>c</sup>*INAF, Osservatorio Astrofisico di Torino, Strada Osservatorio 20, 10025 Pino Torinese, Italy*

<sup>d</sup>*Jodrell Bank Centre for Astrophysics, The University of Manchester, Oxford Road, Manchester M13 9PL, UK*

<sup>e</sup>*Institute Lorentz, Leiden University, PO Box 9506, Leiden 2300 RA, The Netherlands*

<sup>f</sup>*Argelander-Institut für Astronomie, Auf dem Hügel 71, D-53121 Bonn, Germany*

---

## Abstract

Tensions between cosmic microwave background (CMB) observations and the growth of the large-scale structure (LSS) inferred from late-time probes pose a serious challenge to the concordance  $\Lambda$ CDM cosmological model. State-of-the-art CMB data from the *Planck* satellite predicts a higher rate of structure growth than what preferred by low-redshift observables. Such tension has hitherto eluded conclusive explanations in terms of straightforward modifications to  $\Lambda$ CDM, e.g. the inclusion of massive neutrinos or a dynamical dark energy component. Here, we investigate ‘quartessence’ models, where a single dark component mimics both dark matter and dark energy. We show that such models greatly alleviate the tension between high and low redshift observations, thanks to the non-vanishing sound speed of quartessence that inhibits structure growth at late times on scales smaller than its corresponding Jeans’ length. In particular, the  $3.4\sigma$  tension between CMB and LSS observables is thoroughly reabsorbed. For this reason, we argue that quartessence deserves further investigation and may lead to a deeper understanding of the physics of the dark Universe.

---

## 1. Introduction

The current concordance cosmological model owes its name,  $\Lambda$ CDM, to the two most abundant constituents of the present-day Universe: the cosmological constant,  $\Lambda$ , and a (cold) dark matter component. The former, responsible for the late-time accelerated expansion of the cosmos, amounts to  $\sim 70\%$  of the total energy budget; the latter, whose gravitational pull shaped the cosmic large-scale structure (LSS), constitutes more than  $85\%$  of all the matter in the Universe, and roughly a quarter of its total content [1].

Despite the success of the  $\Lambda$ CDM model, a comparison among recent data sets suggests that the agreement between theory and observations is not adamantine. CMB data by *Planck* [1] is in tension with low-redshift observations, e.g. galaxy clustering as inferred through redshift space distortions

(RSD) [2], weak gravitational lensing [3, 4], galaxy cluster counts [5] and local measurements of the Hubble constant,  $H_0$  [6, 7]. Summarising, if we extrapolate CMB data to late times following  $\Lambda$ CDM prescriptions, we will expect a higher rate of structure growth than what favoured by low redshift probes [8, 9].

Various approaches to tackling this serious problem have been adopted, often involving extensions or modifications of the  $\Lambda$ CDM model. Among the most physically motivated attempts, there is the inclusion of a free parameter accounting for the total mass of neutrinos [e.g. 10, 11]. It is known from particle physics that neutrinos have small but non-negligible masses, as well as it is known, in cosmology, that the presence of massive neutrinos during the formation of the LSS causes a damping of matter fluctuations on scales smaller than the neutrino free-streaming length—which, in turn, is related to their masses. Thence the idea of reconciling CMB and LSS data by including massive neutrinos, whose effect will be negligible in the early Universe, although suppressing structure growth at low red-

---

*Email addresses:* [stefano.camera@unito.it](mailto:stefano.camera@unito.it) (Stefano Camera), [martinelli@lorentz.leidenuniv.nl](mailto:martinelli@lorentz.leidenuniv.nl) (Matteo Martinelli), [dbertacca@astro.uni-bonn.de](mailto:dbertacca@astro.uni-bonn.de) (Daniele Bertacca)

shifts. Unfortunately, as shown by Joudaki et al. [11], this scenario turns out not to be viable, mostly because of degeneracies between neutrino masses and other cosmological parameters.

Another possible route is that of dark energy and modified gravity theories [for comprehensive reviews see 12, 13]. As the underlying nature of dark matter and  $\Lambda$  remains utterly unknown, a plethora of models, either phenomenological or emanated from first principles, have been proposed as alternatives to  $\Lambda$ CDM. An interesting family of such unorthodox cosmologies treats  $\Lambda$  and dark matter as two faces of the same entity, a ‘dark component’ that both drives the current accelerated cosmic expansion and is responsible for the growth of the LSS. A large variety of these models—often called ‘unified dark matter’ or ‘quartessence’, in analogy to quintessence dark energy—are based on adiabatic fluids or on scalar field Lagrangians. On this topic, pioneering studies were made by e.g. Refs. [15–17], whereas for a recent review see e.g. Bertacca et al. [18]. Their distinctive feature is the existence of pressure perturbations in the rest frame of the quartessence, effectively originating a Jeans’ length below which the growth of density inhomogeneities is impeded and the evolution of the gravitational potential is characterised by an oscillatory and decaying behaviour [19–30].

## 2. Quartessence models

In this work we consider a particular class of scalar-field quartessence models [18, 22] with Born-Infeld kinetic term [31], whose Lagrangian can be thought as a field theory generalisation of the Lagrangian of a relativistic particle [32–34]. The most important thing to bear in mind here is that these models are indistinguishable from  $\Lambda$ CDM at background level. Furthermore, as is the case of massive neutrinos, there is only one additional parameters with respect to  $\Lambda$ CDM. This parameter,  $c_\infty$ , is related to the effective sound speed of quartessence,  $c_s^2$ , and represents its asymptotic value at  $t \rightarrow \infty$ . Specifically, the speed of sound evolves with redshift according to [22]

$$c_s^2(z) = \frac{\Omega_\Lambda c_\infty^2}{\Omega_\Lambda + (1 - c_\infty^2)\Omega_{\text{DM}}(1+z)^3}. \quad (1)$$

Here, we ‘interpret’  $\Omega_\Lambda$  and  $\Omega_{\text{DM}}$  as the cosmological parameters of the effective cosmological constant and cold dark matter energy density, respectively. Note that this model recovers  $\Lambda$ CDM in the

limit  $c_\infty = 0$ . In other words, the  $\Lambda$ CDM parameter space is an hypersurface of the higher-dimensional parameter space of this family of quartessence models, reason for which we shall from now on use the notation  $\Lambda$ CDM and  $\Lambda$ CDM+ $c_\infty$ . Similarly, we shall later refer to a cosmological model with free neutrino masses as  $\Lambda$ CDM+ $\sum m_\nu$ .

In quartessence, the evolution of the gravitational potential of the LSS is determined by the background and perturbation evolution of quartessence alone. For scales  $k$  smaller than the cosmological horizon and redshift  $z < z_{\text{rec}} \simeq 1000$ , we have  $\delta(k, z) = T_Q(k, z)\delta_m(k, z)$ , where  $\delta_m$  is the matter density perturbation in  $\Lambda$ CDM and  $T_Q$  is the transfer function for the quartessence component. We adopt the approximate functional form [28]

$$T_Q(g) = 2^{5/8}\Gamma\left(\frac{13}{8}\right)g^{-5/8}J_{5/8}(g), \quad (2)$$

where  $g[k, \eta(z)] = \int_{\eta_{\text{rec}}}^{\eta} d\eta' k c_s(\eta')$  and  $\eta$  is the conformal time.

As a result of the modified evolution of density fluctuations when  $c_\infty \neq 0$ , several cosmological observables differ from the  $\Lambda$ CDM expectation. For a start, we can look at galaxies’ peculiar velocities and gravitational lensing distortions induced by the intervening LSS on light emitted by distant sources. To find signatures of a non-vanishing  $c_\infty$ , we therefore analyse currently available measurements of baryon acoustic oscillations and redshift-space distortions from the Sloan Digital Sky Survey (SDSS) DR11 [35–37], and weak lensing cosmic shear from the Kilo-Degree Survey (KiDS) [4, 11].

It is important to notice that, albeit negligible at the time of recombination, the presence of quartessence will also impact observations of the CMB. Indeed, CMB photons are lensed by cosmological structures—an effect leading to a smoothing of the acoustic peaks of CMB spectra. As the larger  $c_\infty$  the more suppressed the growth of matter perturbations, increasing  $c_\infty$  values therefore lead to lower amplitudes of the CMB lensing potential [24, 26]. In turn,  $\Lambda$ CDM+ $c_\infty$  CMB spectra differ from the standard  $\Lambda$ CDM prediction at angular scales corresponding to the acoustic peaks, as shown in Fig. 1. Thanks to this effect, described here for the first time, we can also use CMB data to scrutinise the viability of  $\Lambda$ CDM+ $c_\infty$  models. Hence, we employ temperature and polarisation spectra from the latest *Planck* release [38].

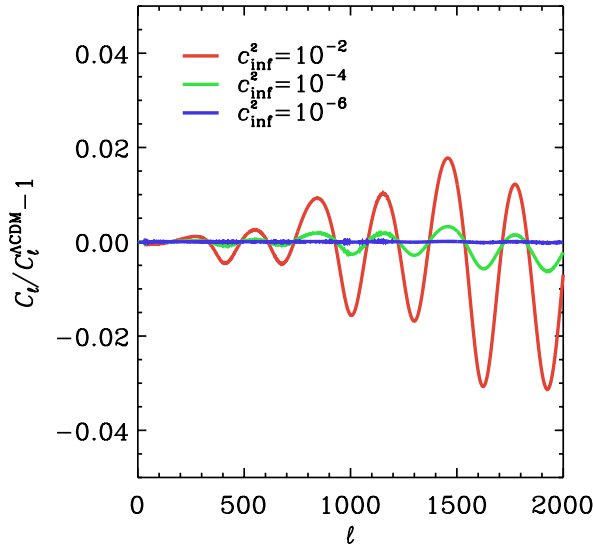


Figure 1: Relative difference between the CMB temperature spectrum in  $\Lambda$ CDM and in the case of a non-vanishing  $c_\infty$ .

### 3. Analysis and results

Summarising, our aim is to state whether or not the non standard clustering of  $\Lambda$ CDM+ $c_\infty$  models can ease the CMB-LSS tension. First, we proceed to quantify the constraints on  $c_\infty$  obtained from CMB and LSS data. For this purpose, we sample the standard  $\Lambda$ CDM 6 parameters set: the baryon and cold dark matter physical densities,  $\omega_b = \Omega_b h^2$  and  $\omega_{\text{DM}} = \Omega_{\text{DM}} h^2$ ; the sound horizon at the last scattering surface,  $\theta_*$ ; the amplitude and tilt of the primordial spectrum of scalar perturbations,  $A_s$  and  $n_s$ ; and the optical depth to recombination,  $\tau$ . To these parameters, we add  $c_\infty$ . For comparison, we also analyse the case of massive neutrinos,  $\Lambda$ CDM+ $\sum m_\nu$ , for which we sample the same cosmological parameter set adding a free value for the sum of neutrino masses,  $\sum m_\nu$  [cfr 10, 39]. The parameter space is sampled assuming flat priors for all the parameters and using Monte-Carlo Markov Chains (MCMC) and a Gelman-Rubin convergence diagnostic implemented in the publicly available code **CosmoMC** [40, 41]. This is interfaced with a version of the public code **CAMB** [42, 43], modified in order to account for a non vanishing  $c_\infty$  by including  $T_Q(k, z)$  of Eq. (2) in **CAMB**'s default DM transfer function.

It is common in literature, for extensions of  $\Lambda$ CDM model affecting the growth of cosmic struc-

tures, to remove from the analysis those scales where non-linear effects are relevant [e.g. 11, 44], in order not to rely on non-linear modelling based on  $\Lambda$ CDM numerical simulations. Here, however, we decide to include such scales, using the corrections to the linear power spectrum computed by the **HMCODE** [45], since even the largest  $c_\infty$  values included will not lead to significant deviations from the standard  $\Lambda$ CDM behaviour at the scales probed by the data [see also 26].

Table 1 shows the results obtained with different data set combinations when only  $c_\infty$  is added to the  $\Lambda$ CDM parameter set. As in the recent literature [4, 11], we also quote constraints on the derived parameter  $S_8 = \sigma_8 \Omega_m^{0.5}$ , which is the combination of  $\sigma_8$ , the rms mass fluctuations on a scale of  $8h^{-1}$  Mpc, and the total matter fraction  $\Omega_m = h^{-2}(\omega_b + \omega_{\text{DM}})$ , mainly constrained by current weak lensing data. The latter is often used as a proxy to exemplify the CMB-LSS tension.

These results highlight how  $c_\infty$  is strongly constrained by LSS observables, while *Planck* alone, which is only affected through CMB lensing, allows for larger values of the parameter, as it can be seen in Figs 2 and 3. This translates into much broader bounds on  $S_8$  from CMB data and with a lower mean value for this parameter combination with respect to the standard  $\Lambda$ CDM bound ( $S_8 = 0.4694 \pm 0.0099$ ), a scenario opposite to the one of  $\Lambda$ CDM+ $\sum m_\nu$  where the neutrino mass is strongly constrained by CMB.

As a result, the CMB-LSS tension can be eased by a  $c_\infty \neq 0$  due to its effect on  $S_8$ , shown in Fig. 3. In the left panel, it is easy to see that larger values of  $c_\infty$  imply a smaller  $S_8$ , thus reconciling high- and low-redshift observations. This can be also appreciated by quantifying the  $S_8$  tension with the estimator proposed by Refs [4, 11]

$$T(S_8) = \frac{|S_8^{\text{CMB}} - S_8^{\text{LSS}}|}{\sqrt{\sigma^2(S_8^{\text{CMB}}) + \sigma^2(S_8^{\text{LSS}})}}, \quad (3)$$

where by ‘CMB’ and ‘LSS’ we indicate that the parameter constraint is obtained from a *Planck* or KiDS+RSD analysis, respectively. For the  $\Lambda$ CDM+ $c_\infty$  model considered here, we obtain  $T_{c_\infty}(S_8) = 0.3$ , therefore the considered model improves the  $3.4\sigma$  tension we find when comparing CMB and LSS data in the standard  $\Lambda$ CDM. This is straightforward to understand from Fig 4, where the  $1\sigma$  error intervals on  $S_8$ , marginalised over all other parameters, from *Planck* (red lines)

Table 1: Marginalised values and  $1-\sigma$  errors on the  $c_\infty$  and  $\sigma_8$  for *Planck*, KiDS and *Planck+KiDS*.

	<i>Planck</i>	LSS	<i>Planck+LSS</i>
$c_\infty$	$(0.1 \pm 3.3) \times 10^{-3}$	$(0.0 \pm 0.37) \times 10^{-3}$	$(0.0 \pm 0.26) \times 10^{-3}$
$S_8$	$0.378^{+0.10}_{-0.039}$	$0.405 \pm 0.016$	$0.4510 \pm 0.0076$

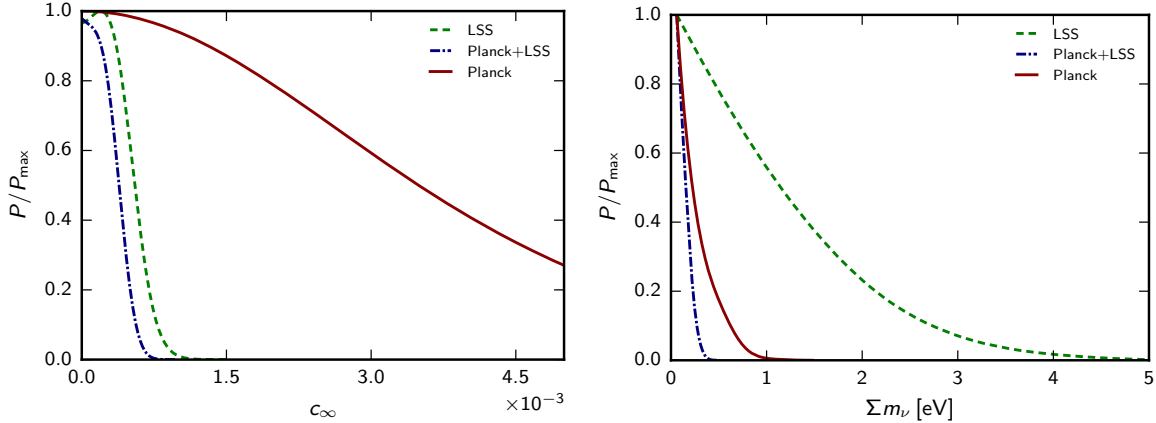


Figure 2: Posterior distributions for  $c_\infty$  (left panel) and  $\sum m_\nu$  (right panel), showing constraints from *Planck* (red, solid lines), LSS observables (green, dashed lines) and the combination of the two (blue, dot-dashed lines).

and KiDS+RSD (green lines) data sets are shown for  $\Lambda$ CDM,  $\Lambda$ CDM+ $c_\infty$  and  $\Lambda$ CDM+ $\sum m_\nu$ .

Figure 5 shows the 2D joint marginal error contours for  $\Omega_m$  and  $\sigma_8$  in standard  $\Lambda$ CDM and for both  $\Lambda$ CDM+ $c_\infty$  and  $\Lambda$ CDM+ $\sum m_\nu$ . It is possible to notice how even though both  $\sum m_\nu$  and  $c_\infty$  are able to ease the  $\sigma_8$  tension (although to a much different extent), their effects are substantially different, thus a joint analysis  $\Lambda$ CDM+ $c_\infty$  +  $\sum m_\nu$  would not significantly change the constraints.

Finally, in order to quantify these result better, we perform a model selection analysis, computing the Deviance Information Criterion (DIC) [46] in order to assess which of the considered models ( $\Lambda$ CDM,  $\Lambda$ CDM+ $c_\infty$  and  $\Lambda$ CDM+ $\sum m_\nu$ ) is favoured by the data. For a given model, the DIC is defined as

$$\text{DIC} \equiv \chi_{\text{eff}}^2(\hat{\vartheta}) + 2p_D, \quad (4)$$

with  $\chi_{\text{eff}}^2(\hat{\vartheta}) = -2 \ln \mathcal{L}(\hat{\vartheta})$ ,  $\hat{\vartheta}$  the parameters vector at the maximum likelihood and  $p_D = \overline{\chi_{\text{eff}}^2(\vartheta)} - \chi_{\text{eff}}^2(\hat{\vartheta})$ , where an average taken over the posterior distribution is implied by the bar. The term  $p_D$  accounts for the complexity of the model, balancing the improvement brought on the goodness of fit  $\chi_{\text{eff}}^2$  by the introduction of additional parameters. We compute  $\Delta\text{DIC}$  for the two extended models, using

the DIC of  $\Lambda$ CDM as a reference; given the definition of Eq. (4), a negative (positive) value of  $\Delta\text{DIC}$  will show that the extended model is favoured (disfavoured) by the data over the reference model. Combining CMB and LSS data sets we find that in  $\Lambda$ CDM+ $c_\infty$   $\Delta\text{DIC} = -0.21$ ; although this results is better than what found for  $\Lambda$ CDM+ $\sum m_\nu$  ( $\Delta\text{DIC} \approx 1$  when combining *Planck* and LSS), no preference for the considered model over the standard  $\Lambda$ CDM cosmology is found. This is due to the fact that LSS tightly constrains  $c_\infty$  to be small and, therefore, the joint CMB+LSS posterior does not deviate much from the one obtained in  $\Lambda$ CDM even though an additional parameter is present.

Therefore, we conclude that the effect of the  $\Lambda$ CDM+ $c_\infty$  model on the growth of structure decreases significantly the tension between the considered data sets, to  $0.3\sigma$  from the  $\Lambda$ CDM  $3.4\sigma$ . However, the comparison of the two models, quantified through the DIC, highlights that data do not significantly prefer the extension we consider in this paper.

Let us emphasise that these conclusions depend on the estimators used to quantify the tension ( $T(S_8)$ ) and to compare the models ( $\Delta\text{DIC}$ ). Our results justify further investigation of quartessence model, which we leave for future work, in order to

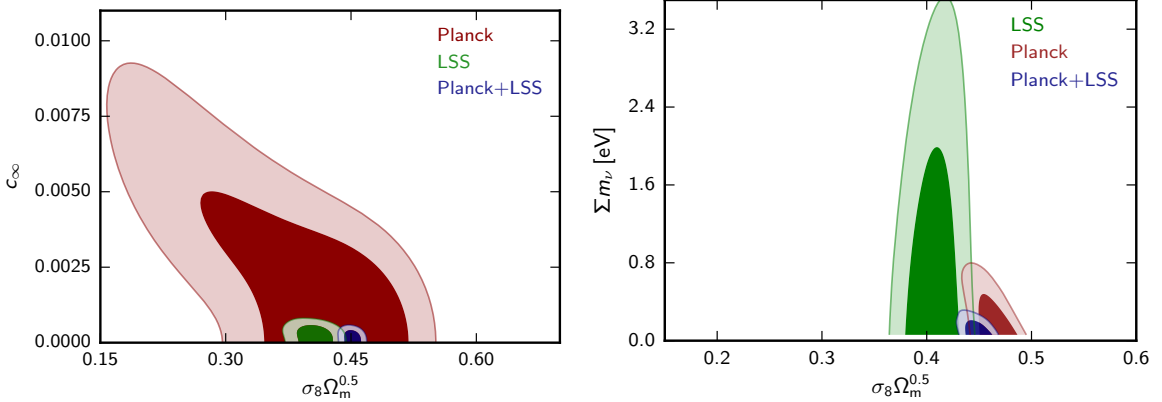


Figure 3: 2D contour plots showing the degeneracy between  $S_8$  and  $c_\infty$  or  $\sum m_\nu$  (left or right panel, respectively), for the various combinations of data sets examined, with darker (lighter) areas depicting 68.3% (95.5%) joint marginal bounds.

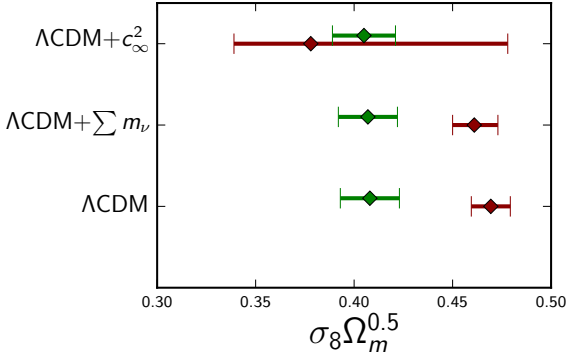


Figure 4: Marginal  $1\sigma$  bounds on  $S_8 = \sigma_8 \Omega_m^{0.5}$  obtained by KiDS+RSD (green lines) and CMB (red lines) data sets in the three cosmological scenarios under investigation.

assess this dependence using other tension estimators [e.g. 47] and more refined model comparison techniques, such as the computation of the Bayesian evidence for the extended model [48]. In any case, we believe that the reconciliation of early- and late-Universe observations attained by quartessence models makes them worth deeper investigations, in particular for what concerns their non-linear behaviour, either with dedicated numerical  $N$ -body simulations or through non-linear perturbation theory approaches.

### Acknowledgements

We thank Anna Bonaldi, Antonaldo Diaferio, Shahab Joudaki and Tom Kitching for valuable support. SC is supported by MIUR through Rita

Levi Montalcini project ‘PROMETHEUS – Probing and Relating Observables with Multi-wavelength Experiments To Help Enlightening the Universe’s Structure’. SC also acknowledges support from ERC Starting Grant No. 280127. MM is supported by the Foundation for Fundamental Research on Matter (FOM) and the Netherlands Organization for Scientific Research / Ministry of Science and Education (NWO/OCW). DB is supported by the Deutsche Forschungsgemeinschaft through the Transregio 33, The Dark Universe.

### References

- [1] P. Ade, et al., Planck 2015 results. XIII. Cosmological parameters .
- [2] E. Macaulay, I. K. Wehus, H. K. Eriksen, Lower Growth Rate from Recent Redshift Space Distortion Measurements than Expected from Planck, Phys. Rev. Lett. 111 (16) (2013) 161301, doi: 10.1103/PhysRevLett.111.161301.
- [3] C. Heymans, et al., CFHTLenS: The Canada-France-Hawaii Telescope Lensing Survey, Mon. Not. Roy. Astron. Soc. 427 (2012) 146, doi:10.1111/j.1365-2966.2012.21952.x.
- [4] H. Hildebrandt, et al., KiDS-450: Cosmological parameter constraints from tomographic weak gravitational lensing doi:10.1093/mnras/stw2805.
- [5] P. A. R. Ade, et al., Planck 2015 results. XXVII. The Second Planck Catalogue of Sunyaev-Zeldovich Sources doi:10.1051/0004-6361/201525823.
- [6] A. G. Riess, L. Macri, S. Casertano, H. Lampeit, H. C. Ferguson, A. V. Filippenko, S. W. Jha, W. Li, R. Chornock, A 3% Solution: Determination of the Hubble Constant with the Hubble Space Telescope and Wide Field Camera 3, Astrophys. J. 730 (2011) 119, doi:10.1088/0004-637X/732/2/129, 10.1088/0004-637X/730/2/119, [Erratum: Astrophys. J.732,129(2011)].

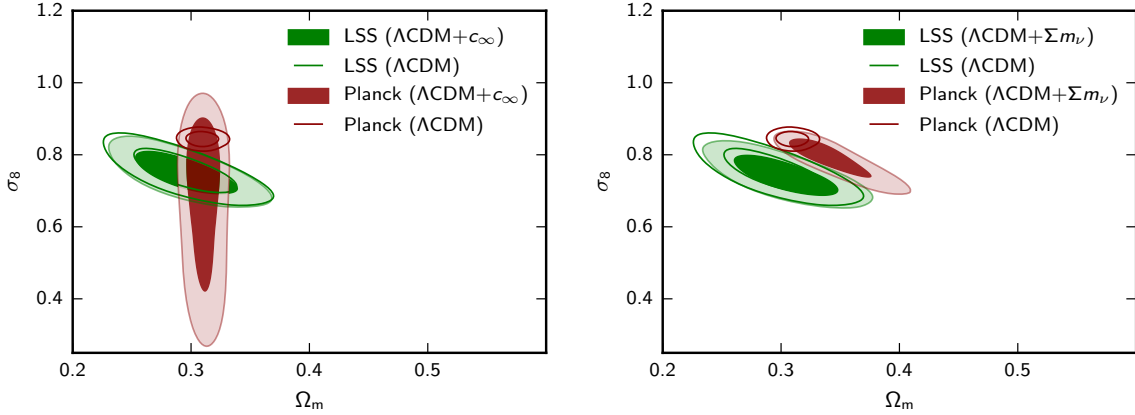


Figure 5: Marginal 1- and 2- $\sigma$  joint error contours in the  $\Omega_m - \sigma_8$  plane obtained by CMB and LSS measurements (red and green contours, respectively). The plot shows the results in  $\Lambda$ CDM (filled contours) and in  $\Lambda$ CDM+ $c_\infty$  and  $\Lambda$ CDM+ $\Sigma m_\nu$  (left and right panel, respectively).

- [7] A. G. Riess, et al., A 2.4% Determination of the Local Value of the Hubble Constant, *Astrophys. J.* 826 (1) (2016) 56, doi:10.3847/0004-637X/826/1/56.
- [8] M. Raveri, Are cosmological data sets consistent with each other within the  $\Lambda$  cold dark matter model?, *Phys. Rev. D* 93 (4) (2016) 043522, doi:10.1103/PhysRevD.93.043522.
- [9] S. Joudaki, et al., CFHTLenS revisited: assessing concordance with Planck including astrophysical systematics .
- [10] R. A. Battye, A. Moss, Evidence for Massive Neutrinos from Cosmic Microwave Background and Lensing Observations, *Phys. Rev. Lett.* 112 (5) (2014) 051303, doi:10.1103/PhysRevLett.112.051303.
- [11] S. Joudaki, et al., KiDS-450: Testing extensions to the standard cosmological model .
- [12] L. Amendola, S. Tsujikawa, *Dark Energy: Theory and Observations*, Cambridge University Press, 2010.
- [13] T. Clifton, P. G. Ferreira, A. Padilla, C. Skordis, Modified Gravity and Cosmology, *Phys. Rept.* 513 (2012) 1–189, doi:10.1016/j.physrep.2012.01.001.
- [14] A. Pourtsidou, T. Tram, Reconciling CMB and structure growth measurements with dark energy interactions, *Phys. Rev. D* 94 (4) (2016) 043518, doi:10.1103/PhysRevD.94.043518.
- [15] V. Sahni, L.-M. Wang, A New cosmological model of quintessence and dark matter, *Phys. Rev. D* 62 (2000) 103517, doi:10.1103/PhysRevD.62.103517.
- [16] A. Yu. Kamenshchik, U. Moschella, V. Pasquier, An Alternative to quintessence, *Phys. Lett. B* 511 (2001) 265–268, doi:10.1016/S0370-2693(01)00571-8.
- [17] N. Bilic, G. B. Tupper, R. D. Viollier, Unification of dark matter and dark energy: The Inhomogeneous Chaplygin gas, *Phys. Lett. B* 535 (2002) 17–21, doi:10.1016/S0370-2693(02)01716-1.
- [18] D. Bertacca, N. Bartolo, S. Matarrese, Unified Dark Matter Scalar Field Models, *Adv. Astron.* 2010 (2010) 904379, doi:10.1155/2010/904379.
- [19] R. J. Scherrer, Purely kinetic k-essence as unified dark matter, *Phys. Rev. Lett.* 93 (2004) 011301, doi:10.1103/PhysRevLett.93.011301.
- [20] D. Giannakis, W. Hu, Kinetic unified dark matter, *Phys. Rev. D* 72 (2005) 063502, doi:10.1103/PhysRevD.72.063502.
- [21] D. Bertacca, N. Bartolo, ISW effect in Unified Dark Matter Scalar Field Cosmologies: an analytical approach, *JCAP* 0711 (2007) 026, doi:10.1088/1475-7516/2007/11/026.
- [22] D. Bertacca, N. Bartolo, A. Diaferio, S. Matarrese, How the Scalar Field of Unified Dark Matter Models Can Cluster, *JCAP* 0810 (2008) 023, doi:10.1088/1475-7516/2008/10/023.
- [23] O. F. Piattella, D. Bertacca, M. Bruni, D. Pietrobon, Unified Dark Matter models with fast transition, *JCAP* 1001 (2010) 014, doi:10.1088/1475-7516/2010/01/014.
- [24] S. Camera, D. Bertacca, A. Diaferio, N. Bartolo, S. Matarrese, Weak lensing signal in unified dark matter models, *Mon. Not. Roy. Astron. Soc.* 399 (2009) 1995–2003, doi:10.1111/j.1365-2966.2009.15326.x.
- [25] D. Bertacca, M. Bruni, O. F. Piattella, D. Pietrobon, Unified Dark Matter scalar field models with fast transition, *JCAP* 1102 (2011) 018, doi:10.1088/1475-7516/2011/02/018.
- [26] S. Camera, T. D. Kitching, A. F. Heavens, D. Bertacca, A. Diaferio, Measuring Unified Dark Matter with 3D cosmic shear, *Mon. Not. Roy. Astron. Soc.* 415 (2011) 399–409.
- [27] D. Bertacca, A. Raccanelli, O. F. Piattella, D. Pietrobon, N. Bartolo, et al., CMB-Galaxy correlation in Unified Dark Matter Scalar Field Cosmologies, *JCAP* 1103 (2011) 039, doi:10.1088/1475-7516/2011/03/039.
- [28] O. F. Piattella, D. Bertacca, Gravitational potential evolution in Unified Dark Matter Scalar Field Cosmologies: an analytical approach, *Mod. Phys. Lett. A* 26 (2011) 2277–2286, doi:10.1142/S0217732311036723.
- [29] S. Camera, C. Carbone, L. Moscardini, Inclusive Constraints on Unified Dark Matter Models from Future Large-Scale Surveys, *JCAP* 1203 (2012) 039, doi:10.1088/1475-7516/2012/03/039.
- [30] A. Raccanelli, D. Bertacca, D. Pietrobon, F. Schmidt, L. Samushia, N. Bartolo, O. Dore, S. Matarrese, W. J.

Percival, Testing Gravity Using Large-Scale Redshift-Space Distortions doi:10.1093/mnras/stt1517.

[31] M. Born, L. Infeld, Foundations of the new field theory, Proc. Roy. Soc. Lond. A144 (1934) 425–451.

[32] T. Padmanabhan, T. Choudhury, Can the clustered dark matter and the smooth dark energy arise from the same scalar field?, Phys. Rev. D66 (2002) 081301, doi:10.1103/PhysRevD.66.081301.

[33] L. R. W. Abramo, F. Finelli, Cosmological dynamics of the tachyon with an inverse power-law potential, Phys. Lett. B575 (2003) 165–171, doi:10.1016/j.physletb.2003.09.065.

[34] L. R. Abramo, F. Finelli, T. S. Pereira, Constraining Born-Infeld models of dark energy with CMB anisotropies, Phys. Rev. D70 (2004) 063517, doi:10.1103/PhysRevD.70.063517.

[35] A. J. Ross, L. Samushia, C. Howlett, W. J. Percival, A. Burden, M. Manera, The clustering of the SDSS DR7 main Galaxy sample - I. A 4 per cent distance measure at  $z = 0.15$ , Mon. Not. Roy. Astron. Soc. 449 (1) (2015) 835–847, doi:10.1093/mnras/stv154.

[36] L. Anderson, et al., The clustering of galaxies in the SDSS-III Baryon Oscillation Spectroscopic Survey: baryon acoustic oscillations in the Data Releases 10 and 11 Galaxy samples, Mon. Not. Roy. Astron. Soc. 441 (1) (2014) 24–62, doi:10.1093/mnras/stu523.

[37] L. Samushia, et al., The clustering of galaxies in the SDSS-III Baryon Oscillation Spectroscopic Survey: measuring growth rate and geometry with anisotropic clustering, Mon. Not. Roy. Astron. Soc. 439 (4) (2014) 3504–3519, doi:10.1093/mnras/stu197.

[38] N. Aghanim, et al., Planck 2015 results. XI. CMB power spectra, likelihoods, and robustness of parameters, Submitted to: Astron. Astrophys. .

[39] R. A. Battye, T. Charnock, A. Moss, Tension between the power spectrum of density perturbations measured on large and small scales, Phys. Rev. D91 (10) (2015) 103508, doi:10.1103/PhysRevD.91.103508.

[40] A. Lewis, S. Bridle, Cosmological parameters from CMB and other data: A Monte Carlo approach, Phys. Rev. D66 (2002) 103511, doi:10.1103/PhysRevD.66.103511.

[41] A. Lewis, Efficient sampling of fast and slow cosmological parameters, Phys. Rev. D87 (10) (2013) 103529, doi:10.1103/PhysRevD.87.103529.

[42] A. Lewis, A. Challinor, A. Lasenby, Efficient computation of CMB anisotropies in closed FRW models, Astrophys. J. 538 (2000) 473–476, doi:10.1086/309179.

[43] C. Howlett, A. Lewis, A. Hall, A. Challinor, CMB power spectrum parameter degeneracies in the era of precision cosmology, JCAP 1204 (2012) 027, doi:10.1088/1475-7516/2012/04/027.

[44] P. Ade, et al., Planck 2015 results. XIV. Dark energy and modified gravity .

[45] A. J. Mead, J. A. Peacock, C. Heymans, S. Joudaki, A. F. Heavens, An accurate halo model for fitting non-linear cosmological power spectra and baryonic feedback models, MNRAS 454 (2015) 1958–1975, doi:10.1093/mnras/stv2036.

[46] D. J. Spiegelhalter, N. G. Best, B. P. Carlin, A. van der Linde, The deviance information criterion: 12 years on, Journal of the Royal Statistical Society: Series B (Statistical Methodology) 76 (3) (2014) 485–493, ISSN 1467-9868, doi:10.1111/rssb.12062, URL <http://dx.doi.org/10.1111/rssb.12062>.

[47] T. Charnock, R. A. Battye, A. Moss, Planck confronts large scale structure: methods to quantify discordance .

[48] A. Heavens, Y. Fantaye, E. Sellentin, H. Eggers, Z. Hosenie, S. Kroon, A. Mootoovaloo, No evidence for extensions to the standard cosmological model .